


## Micrographia

# Ultrastructural Characterization of Salivary Glands, Alimentary Canal and Malpighian Tubules of the Red Shield Bug *Carpocoris mediterraneus* Tamanini, 1958 (Heteroptera, Pentatomidae)

Nurcan Özyurt Koçakoğlu\*  and Selami Candan

Department of Biology, Science Faculty, Gazi University, Ankara 06500, Turkey

### Abstract

In this study, the gut structure and excretory system of *Carpocoris mediterraneus* which is phytophagous insect, were described with light and electron microscopies and discussed in relation to other Heteroptera species. The salivary system has two principal and accessory salivary glands, two principal and accessory gland ducts. The salivary gland and duct wall have a single layer of cuboidal cells. The duct lumen is surrounded by a thick intima layer. In the cytoplasm of the epithelial cells are seen vesicles. The gut includes fore, mid, and hindguts. The foregut consists of a long narrow tubular pharynx which opens into a slightly wider esophagus. The esophagus is thin walled and in turn opens into the midgut. The midgut has four regions (V1–V4). V1–V4 walls have a monolayered epithelium. V1 epithelium is double-nucleated. V1 cytoplasm contains numerous vesicles, secretory granules, spherocrystals, and cytoplasmic inclusions. Rod-shaped bacteria are seen in V4 lumen. The hindgut has pylorus and rectum. Malpighian tubules were attached in the pylorus. Malpighian tubules have a single-layer cuboidal epithelium. In their lumen, there are spherocrystals. The rectum wall has a monolayer of squamous epithelium and muscle layer. Numerous bacteria and uric acid crystals are seen in its lumen.

**Key words:** digestive system, electron microscopy, excretory system, light microscopy, salivary glands

(Received 12 October 2021; revised 7 February 2022; accepted 18 February 2022)

### Introduction

The Pentatomidae family, most of which are phytophages, is one of the largest family of Heteroptera, with 906 genera and 4,700 species in the world, and 54 genera and 162 species in Turkey (Önder et al., 2006). They feed by sucking plant juices from immature fruits and seeds with stylet mouthparts, and many are recognized as pests of food crops (Önder & Lodos, 1986). *C. mediterraneus* Tamanini, 1958 (Pentatomidae) feeds with seeds of Compositae, Graminae, Umbelliferae (Fent & Aktaş, 1999). *C. mediterraneus* causes serious damage when the number of species increases.

Heteroptera have different dietary habits with phytophagous, zoophagous, and hematophagous species, and this dietary diversity associated with the monophyly of Heteroptera makes these insects a good object for digestive system studies (Santos et al., 2017). For zoophagy and phytophagy, Heteroptera saliva compounds contribute to the understanding of the extra-oral digestion of these insects (Baptist, 1941; Ammar, 1986; Nunes & Camargo-Mathias, 2006; Anê et al., 2021; Carvalho et al., 2021; Özyurt Koçakoğlu, 2021). The salivary glands are usually situated in the thorax lying on either side of the gut, but may

lie in the head and may extend into the abdomen. They may be relatively simple or complexly branched and convoluted. It can be said that the salivary system in all Heteroptera consists of a pair of principal and accessory salivary glands. The principal glands are fundamentally bilobed, comprising anterior and posterior lobes. The accessory salivary gland opens through its duct into the hilus of the principal salivary gland (Baptist, 1941).

In insects, including Heteroptera, the alimentary canal is between the mouth and anus and consists of three regions (a) the foregut, which stores, filters, and partially digests food; (b) the midgut, where digestion and absorption takes place, and (c) the hindgut, which functions in water absorption and homeostasis. The foregut and hindgut are lined with the cuticle, while the midgut is devoid of this structure (Candan et al., 2021; Dantas et al., 2021; Özyurt Koçakoğlu & Candan, 2021; Özyurt Koçakoğlu, 2021). In insect, the foregut generally consists of the buccal cavity, the pharynx, the esophagus, the crop (stores food), and the proventriculus or gizzard (grinds food). However, insects with piercing-sucking mouth type such as Heteroptera feed on plant sap, and they do not have crops (Özyurt Koçakoğlu, 2021). The midgut usually makes up the longest part of the gut and is sometimes referred to as the ventriculus or stomach (Kasap, 1979). The hindgut, which is the third region of the digestive system, generally consists of three parts: ileum, colon, and rectum in insect (Gullan & Cranston, 2005). However, in Heteroptera, the hindgut consists of two parts, the

\*Corresponding author: Nurcan Özyurt Koçakoğlu, E-mail: [nurcanozyurt@gazi.edu.tr](mailto:nurcanozyurt@gazi.edu.tr)

Cite this article: Özyurt Koçakoğlu N, Candan S (2022) Ultrastructural Characterization of Salivary Glands, Alimentary Canal and Malpighian Tubules of the Red Shield Bug *Carpocoris mediterraneus* Tamanini, 1958 (Heteroptera, Pentatomidae). *Microsc Microanal* 28, 824–836. doi:10.1017/S1431927622000307

pylorus and the rectum (Özyurt Koçakoğlu, 2021). Malpighian tubules may appear to arise from the midgut, but they actually insert between the midgut and hindgut as ectodermal evaginations of the hindgut (Klowden, 2007). Malpighian tubules are the main organs of osmoregulation and excretion (Gullan & Cranston, 2005).

The heteropteran pests are often managed by the application of various insecticides in agro-ecosystems but have a deleterious effect on nontarget species and host plant (Gangurde et al., 2019). Morphological studies of the alimentary canal are important for understanding the basic organization and will be useful in comparative studies of alimentary canal of individuals reared in different conditions, exposed to stressors such as pesticides, and closely related species. Therefore, to control against *C. mediterraneus*, it is necessary to know the structure of the digestive system of this insect. This study aims to describe the anatomical, histological, and ultrastructural structure of the digestive system of *C. mediterraneus* and to contribute to the knowledge of digestive system biology to species of Pentatomidae and other families. In addition, this study forms the basis for studies to be carried out on the biological control of this species.

## Material and Methods

Twenty adult *C. mediterraneus* were collected in Aksu, Antalya, Turkey, in June 2018. They were kept in the laboratory of Gazi University at 25°C and in perforated plastic jars with plants from their environment.

### Light Microscopy

Firstly, the 20 adult *C. mediterraneus* were dissected under a stereo microscope (SM) within a 0.1 M sodium phosphate buffer solution (pH 7.2). After, five samples were treated with 10% formaldehyde fixation for 24 h and were washed with tap water for 24 h. Next, they were dehydrated in graded ethanol solutions and cleared in series of xylene solutions mixed with paraffin. Then they were kept in pure paraffin for 48 h at 65°C and finally were embedded in paraffin. Paraffin blocks were serially sectioned to a thickness of 6–7 µm with Microm HM 310 microtome (Walldorf, Germany) and mounted on glass slides. The stained sections with hematoxylin and eosin were analyzed under an Olympus BX-51 light microscope (Olympus Corporation, Tokyo, Japan).

### Scanning Electron Microscopy

Five adult samples were fixed in 2.5% glutaraldehyde for 24 h in a 0.1 M sodium phosphate buffer solution (pH 7.2). Then they were rinsed in the same buffer for three times and next dehydrated in a series of ethanol solutions. Ethanol was replaced with Hexamethyldisilazane (HMDS) and samples were dried in air. They were mounted on microscope slides and sputter-coated with gold and examined with a JSM-6060 LV SEM (JEOL, Ltd., Japan) operating at 10 kV.

### Transmission Electron Microscopy

Ten adult samples were fixed with 2.5% glutaraldehyde for 24 h in a 0.1 M sodium phosphate buffer solution (pH 7.4). After they were washed in a solution, the material was postfixed for 2 h in 1% OsO<sub>4</sub> in the same buffer (4°C), dehydrated in graded series of ethanol solutions and propylene oxide and then embedded in an Araldit. Ultrathin sections were cut on a Leica EM UC 6

ultramicrotome. The sections were stained with lead citrate and uranyl acetate, and then washed in distilled water. Then, some of ultrathin sections were examined with a JEOL JEM 1400 TEM at 80 kV in Gazi University. Other sections were recorded at Ankara University in a JEOL JEM-100CX II TEM again at 80 kV.

## Results

### Salivary Glands

The salivary system of *C. mediterraneus* consists of a pair of principal salivary glands, a pair of accessory salivary glands, a pair of principal gland ducts, and a pair of accessory gland ducts. The salivary glands empty by means of a long duct which extends into the head capsule. Each principal salivary gland consists of two lobes, anterior and posterior lobes and with striking differences in size and form. The anterior lobe was located close to the foregut and shorter than the posterior lobe. The anterior lobe of principal glands runs parallel to the pharynx and esophagus on either side of the pharynx and esophagus (Fig. 1a). The anterior lobe of the principal salivary gland is narrow distally, but widens proximally. It has a pear-shaped appearance (Figs. 1a, 1b). Posterior lobe of principal salivary glands lies on either side of midgut (Figs. 1a, 1b). The posterior lobe is wide sac proximally and narrow distally (Figs. 1b–1d). The anterior lobe is smaller than the posterior one (Figs. 1a–1d). The surface of the proximal part of posterior lobe has smooth surface (Fig. 1d), and the distal part of posterior lobe has a blistered appearance (Figs. 1e, 1f).

The hilus is distinguished between the anterior lobe and the posterior lobe of the principal salivary gland (Fig. 1d). The ducts of the principal and accessory gland connect to the hilus region. The accessory gland duct, which forms large S-shaped folds, and the principal gland duct, which extends more straight, are connected to the hilus part (Fig. 1d).

The principal gland duct is connected with the salivary duct of the other principal salivary gland to form a single salivary duct that opened in the mouthpart stylet inside the head. Histologically, the anterior and posterior lobes of the principal salivary gland are similar (Fig. 1c). The principal salivary gland wall is surrounded by a single layer of cuboidal cells. The epithelial cell cytoplasm is basophilic (Figs. 1c, 1e). The cuticle coating the lumen of the principal salivary gland is not present (Figs. 1c, 1e). The secretion texture is acidophilic and granulous (Fig. 1e). In the sections taken from the distal end of the posterior lobe of the principal gland, it is distinguished that the epithelial cells are folding toward the lumen, and numerous secretion vesicles are seen in the lumen (Fig. 1e). In the middle of each cell, there is a large and round nucleus (Fig. 1e). The TEM photograph shows that the nucleus of the principal salivary gland epithelial cell is large and irregular in shape (amoeba-shape) with fine extensions into the cytoplasm and it has predominance of condensed chromatin clusters (Fig. 2a). Numerous granulated endoplasmic cisternae with electron-lucent content and mitochondria are seen in epithelial cells (Fig. 2b). In the median cell region, there are electron-lucent structures and small electron-dense granules characteristic of glycogen deposits (Fig. 2c). In TEM examinations, the muscle layer surrounding the epithelium of the principal salivary gland is distinguished (Fig. 2d).

The wall of the accessory salivary gland is surrounded by a monolayer cubic epithelium (Fig. 3a). It is distinguished that the accessory salivary gland consists of 5–6 cells in its cross-sections, and the lumen is narrow (Fig. 3b). In *C. mediterraneus*,

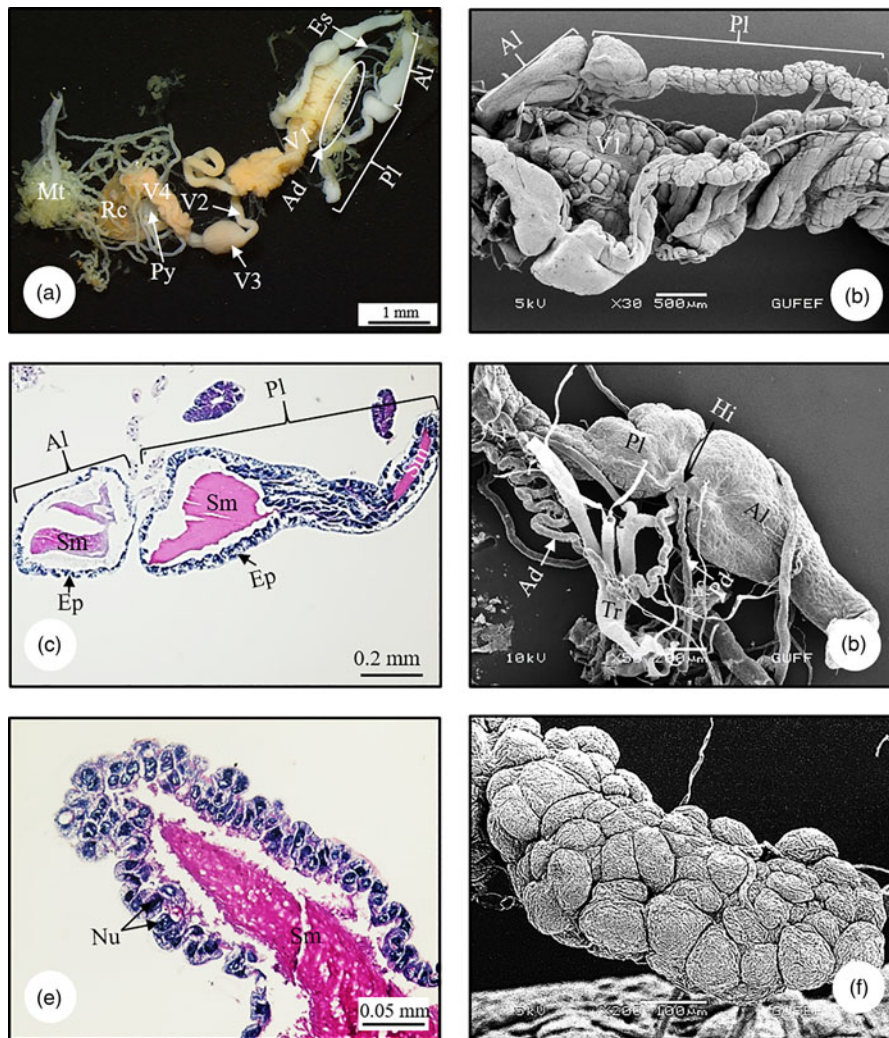


**Fig. 1.** (a) General view of the salivary gland, alimentary canal in *C. mediterraneus* (SM). (b) SEM photograph of anterior and posterior lobes forming the principal salivary gland. (c) The histological section anterior and posterior lobes in principal salivary gland (LM). (d) SEM photo of accessory gland duct and principal duct, anterior lobe, posterior lobe forming salivary gland. (e) The longitudinal section of posterior lobe of principal salivary gland (LM). (f) SEM photograph of the distal end of the posterior lobe in the principal salivary gland. Ad, accessory gland duct; Al, anterior lobe; Ep, epithelium; Es, esophagus; Hi, hilus; Mt, malpighian tubule; Pl, posterior lobe; Py, pylorus; Rc, rectum; Sm, secretory material; V1, ventriculus 1; V2, ventriculus 2; V3, ventriculus 3; V4, ventriculus 4.

the accessory gland of salivary gland is tubular (Fig. 3b). Histological sections and SEM photographs show that the cell contents are filled with secretory granules (Fig. 3b). TEM photographs of the accessory salivary gland show that the cell has round nuclei that are less dense in chromatin, there are many mitochondria and secretory granules in the cytoplasm of epithelial cells, and lateral membrane folding between cells (Figs. 3c, 3d).

The accessory gland duct has a thin, long, S-shaped curved appearance (Fig. 4a). In the SEM and LM photographs, its lumen is quite narrow, its wall is surrounded by a thick intima layer from the lumen, a simple cubic epithelium with round, large, and basophilic nuclei in the middle of the cell (Figs. 4b–4d). The cytoplasm of the epithelial cells of the accessory gland duct has vesicles in different sizes with electron-lucent content (Fig. 4e). The accessory gland duct cells contain apical membrane foldings under the cuticula layer (Fig. 4e). The basal region of cells in the accessory gland duct are characterized by plasma membrane infoldings, which are associated with mitochondria and extend across 1/3 of the cell (Fig. 4f).

### Alimentary Canal

The digestive system of *C. mediterraneus* is divided into three regions: foregut, midgut, and hindgut. The foregut consists of the pharynx and esophagus. The midgut has four regions as first, second, third, and four ventriculi. The hindgut consists of the pylorus and rectum (Fig. 1a).

### Foregut

The foregut consists of a long narrow tubular pharynx which opens into a slightly wider esophagus. The esophagus is thin walled and in turn opens into the V1 (Fig. 1a).

### Midgut

Midgut consists of four separate ventriculus regions as V1–V4. In SM and SEM photographs, it is distinguished that the V1 surface is not flat but has large folds and its surface has the appearance of

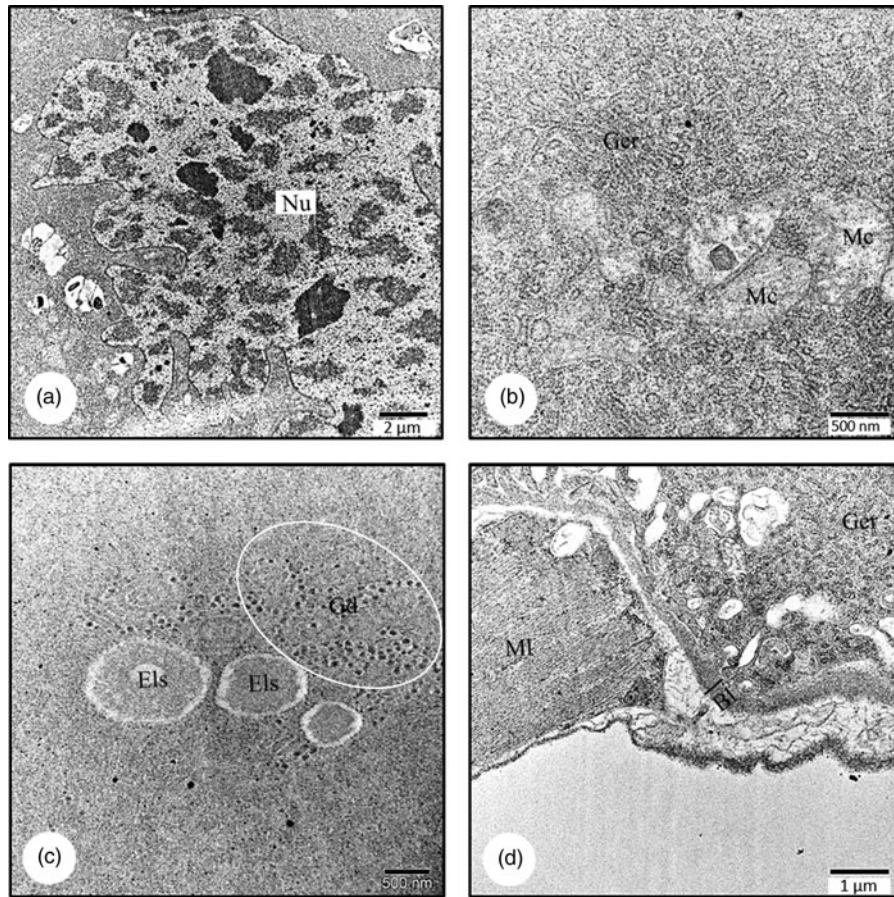


**Fig. 2.** (a) TEM photograph of the nucleus which is large and irregular in shape with fine extensions into the cytoplasm of principal salivary gland in *C. mediterraneus*. (b) Numerous granulated endoplasmic reticulum and mitochondria in epithelial cells (TEM). (c) The electron-lucent structures and small electron-dense granules in the median cell region (TEM). (d) The muscle layer surrounding the epithelium of the principal salivary gland (TEM). Bl, basal lamina; Els, electron-lucent structures; Gd, granules; Ger, granulated endoplasmic cisternae; Mc, mitochondria; MI, muscle layer; Nu, nucleus.

a bubble (Figs. 5a, 5b). Anatomically, longitudinal muscles are seen on the surface of V1 (Fig. 5b). In the LM and SEM photographs, it is observed that the V1 wall is surrounded by a double-nucleated, monolayered epithelium with round nuclei and sheath (Figs. 5c, 5d). The cells have an apical border of microvilli (Fig. 5d). The epithelium has deep folds toward the lumen (Fig. 5c). These folds increase the surface area of the epithelium and increase absorption. In ultrastructural examinations, the cytoplasm of epithelial cells contains numerous vesicles, golgi complexes, spherocrystals, and cytoplasmic inclusions (Figs. 5e, 5f). There is thin muscle layer surrounding the epithelium. The nucleus of the muscle tissue is irregular (amoeba-shape) (Fig. 5e). In SEM photographs, it is distinguished that V2 has a long channel structure, its surface is surrounded by muscles (Fig. 6a). The histological sections of V2 show that it is surrounded by a monolayer cylindrical epithelium with a round nucleus in the middle, and a thin muscle layer. Also, there are secretory sacs around the apical region of epithelial cells (Fig. 6b). In TEM photographs of V2, monolayered cylindrical epithelial cells lined up on the basal lamina are distinguished. Epithelial cells are surrounded by a thin muscle layer, and tracheae are found in places. The nucleus of the cell is less dense in chromatin, and the nucleolus is seen near the center (Fig. 6c). Microvilli extend from the apices of the epithelial cells and show a regular arrangement. There are numerous mitochondria in the cytoplasm of the epithelial cell (Fig. 6d). V3, the third

region of the midgut, is transparent in color and has the shape of a bulging, rounded sac. The surface is quite flat (Fig. 7a). The lumen is quite large and its contents are filled with secretory material (Fig. 7b). The wall of V3 is surrounded by a muscle layer and a monolayer cylindrical epithelium with round nuclei at the center (Fig. 7b). In the lumen, there are secretory materials and granules released from the secretory cells. These digestive cells release their secretions through the plasma membrane producing membrane-bound vesicles in the lumen (Fig. 7b). These secretions are seen as the release of secretory materials accompanied with partial loss of cytoplasm. This secretion release type is apocrine. In the TEM micrographs of V3, the cell has round nuclei with heterochromatin clusters, regularly arranged microvilli at the apical part of the epithelial cells, and secretory vesicles in the cytoplasm of the cell, which merge with each other in numerous clusters (Figs. 7c, 7d). V4 consists of four channels that connect to the pylorus region of the hindgut (Figs. 8a, 8b). V4 has a transverse gnarled structure (Fig. 8c). The duct of V4 is also seen as flat sacs lined with a monolayer of epithelium (Fig. 8d). Rod-shaped bacteria in the lumens of V4 that aid digestion are seen in SEM and TEM photographs (Figs. 8e, 8f). In ultrastructural examinations, V4 epithelial cells are located on the basal lamina, basal membrane folds are not observed, numerous vesicles and mitochondria are distinguished in the cytoplasm of the epithelium (Fig. 8f). The pylorus provides the attachment of the V4 and the insertion of Malpighian tubules.

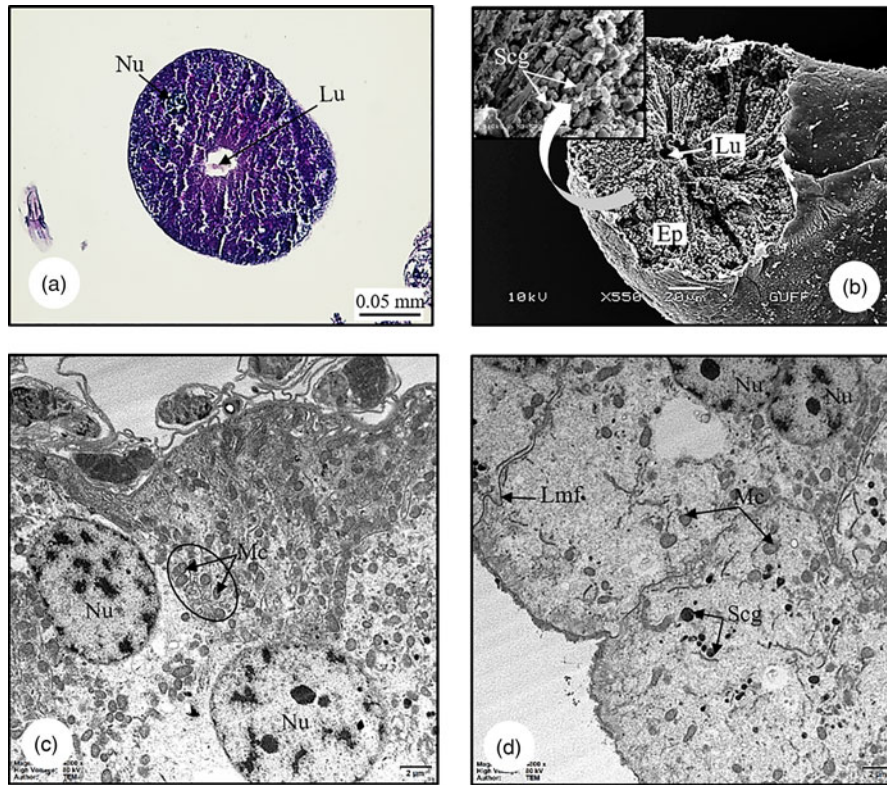


**Fig. 3.** (a,b) LM and SEM photographs of cross-section of accessory salivary gland in *C. mediterraneus*. (c,d) TEM photographs of accessory salivary gland. Ep, epithelium; Lmf, lateral membrane folding; Lu, lumen; Mc, mitochondria; Nu, nucleus; Scg, secretory granules.

### Malpighian Tubules

Malpighian tubules were attached in the pylorus (Fig. 9a). Each Malpighian tubule has two morphologically distinct regions. The first part (the proximal region of Malpighian tubules) which opens into the pylorus, has a flat surface and white in color (Fig. 9a). The second part (the distal region of Malpighian tubules) is blinded and free in the hemocoel, it appears as a double string of beads, and is light yellow in color (Figs. 9a, 9b). The Malpighian tubules of *C. mediterraneus* consist of a single layer cuboidal epithelium with a few cells surrounding the lumen (Figs. 9c–9f). The cell nuclei, which are oval or spherical in shape, are found in the basal of the cells (Figs. 9d–9f). In light microscopy, SEM, and TEM photographs, there is a brush border on the apex of the cells (Fig. 9e). In some regions of the Malpighian tubules, the length of the microvilli is about one-third the width of the epithelium (Fig. 9g). In the cytoplasm of Malpighian tubule cells, there are numerous vesicles in various sizes and some have connections (Figs. 9g–9i). The vesicles appear larger toward the basement membrane, while smaller toward the perinuclear area (Fig. 9g). In the lumen, there are spherocrystals (mineral concretions) surrounded by an electron-dense lamellar layer (Fig. 9h). Microvilli extending from the apical part of the epithelial cells are distinguished (Fig. 9j).

### Hindgut

The pylorus is the part where the substances coming from V4 and Malpighian tubules are collected (Fig. 9a). In the LM photographs, the pylorus wall is surrounded by a monolayer cylindrical epithelium with a striated border at the apical part, and a thin layer of muscle layer (Fig. 10a). Epithelial cells have dark, basophilic nuclei

in the middle of the cells (Fig. 10a). In TEM examinations of pylorus region, basal membrane folds are observed in the basal part of the epithelial cells and short microvilli in the apical part. The nuclei of their cells have a recessed-protruding shape, and heterochromatin parts are few in the nucleus. There are many mitochondria in the cytoplasm of epithelial cells. There is a wide gap between the basal lamina and the epithelium. The muscle layer is seen outside the basal lamina (Fig. 10b).

The pylorus joins with the oval sac shaped rectum, which is the last part of the hindgut and opens to the exterior at the anus. Histologically, the rectum wall is surrounded by a monolayer of squamous epithelium and muscle layer. Epithelial cells are zigzag-shaped and have oval-round nuclei. The epithelium has deep folds toward the lumen (Fig. 11a). In SEM photographs, it is observed that the rectum of *C. mediterraneus* is in the form of a sac, its surface is covered with longitudinal muscles (Fig. 11b), and there is an intima layer with folds on the inner surface of the rectum wall (Fig. 11c). Numerous bacteria and square-shaped uric acid crystals are seen in the lumen of the rectum in SEM and TEM photographs (Figs. 11d–11f). A great deal of foldings at the lateral plasma membrane is observed. In ultrastructural studies, it is distinguished that the nucleus is less dense in euchromatin. Epithelial cells have numerous mitochondria in their cytoplasm (Fig. 11e).

### Discussion and Conclusion

#### Salivary Glands

The salivary system of *C. mediterraneus* has a pair of principal and accessory salivary glands and ducts (principal and accessory

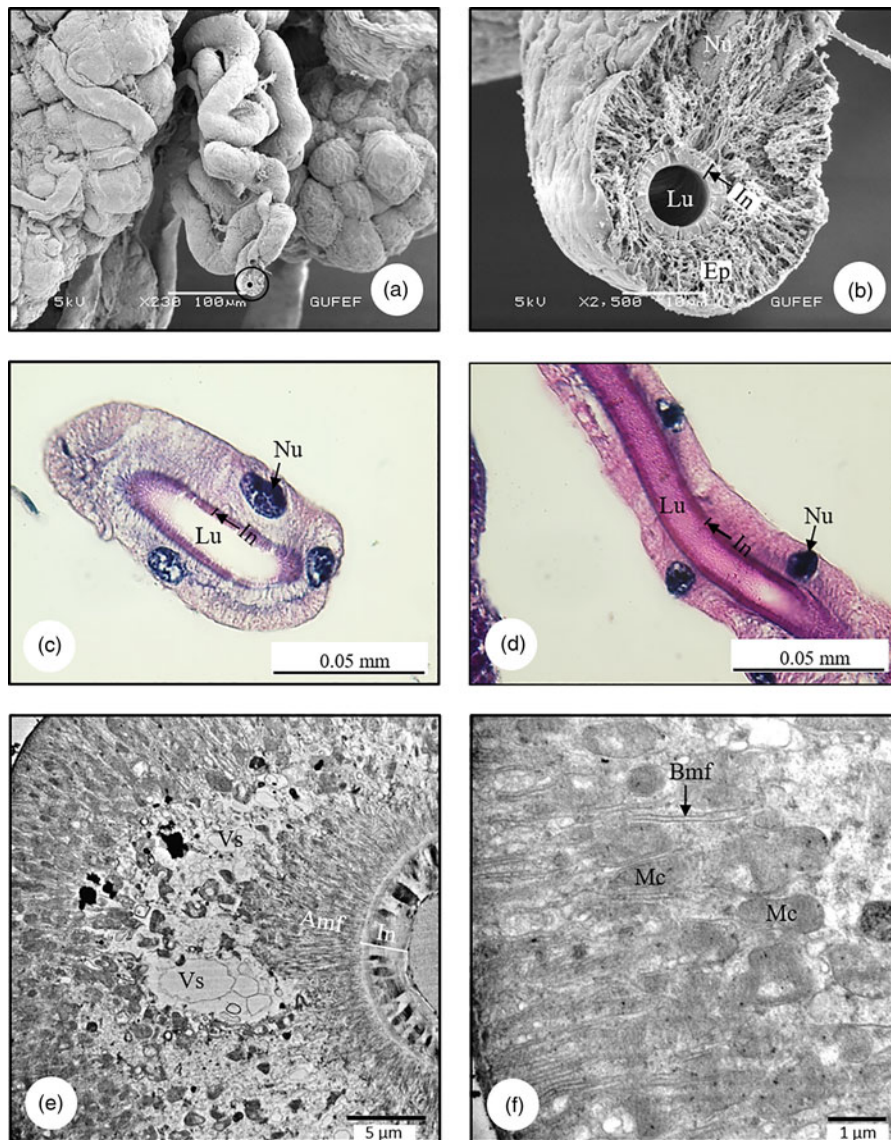


**Fig. 4.** (a) SEM photograph of accessory gland duct with curved appearance in *C. mediterraneus*. (b) The intima and epithelium surrounding accessory gland duct (SEM). (c,d) The cross and longitudinal sections of intima and epithelium surrounding accessory gland duct (LM). (e) TEM photograph of vesicles in different sizes with electron-lucent content in accessory gland duct cells. (f) Mitochondria between basement membrane folds (TEM) in accessory gland duct cells. Amf, apical membrane folding; Bmf, basal membrane folding; Ep, epithelium; In, intima; Lu, lumen; Mc, mitochondria; Nu, nucleus; Vs, vesicle.

gland ducts), as in *Solubea pugnax* (Fabricius) (Pentatomidae; Hamner, 1936), *Brontocoris tabidus* (Signoret) (Pentatomidae; Azevedo et al., 2007; Carvalho et al., 2021), *Euschistus heros* (Fabricius) (Pentatomidae; Castellanos et al., 2017), and *Rhodnius prolixus* Stål, 1859 (Reduviidae; Anhê et al., 2021).

In *C. mediterraneus*, principal salivary gland has two lobes as anterior and posterior lobes, as in *S. pugnax* (Pentatomidae; Hamner, 1936), *E. heros* (Pentatomidae; Castellanos et al., 2017), *Scaptocoris castanea* Perty, 1830 (Cydnidae; Cossolin et al., 2019) and *B. tabidus* (Pentatomidae; Carvalho et al., 2021). In *Metacanthus elegans* L. (Berytidae), *Chilacis typhae* Perr (Lygaeidae), and *Gastrodes ferrugineus* L. (Lygaeidae), principal gland is trilobed with anterior, posterior, and lateral lobes (Baptist, 1941). However, in some species, lobe numbers of principal salivary gland vary. *Pyrrhocoris apterus* (Linnaeus, 1758) (Pyrrhocoridae) have a quadrilobed principal gland as anterior, posterior, median, and lateral lobes (Baptist, 1941; Özyurt

Koçakoğlu, 2021). The number of principal salivary gland lobes differs according to the species.

The shape of the principal gland in insects varies among different species. The anterior lobe of the principal gland in *C. mediterraneus* is a pear-shaped, but the posterior lobe of the principal gland is wide proximally and long and narrow distally. However, in *S. pugnax* (Pentatomidae), the anterior lobe of the principal salivary gland has four prominent finger-shaped projections and the posterior lobe is tubular (Hamner, 1936). In *E. heros* (Pentatomidae), while the anterior lobe is semi-oval with four irregular projections of different sizes, the posterior lobe is elongated and takes an oval shape with small projections in the proximal lobe (Castellanos et al., 2017). In *S. castanea* (Cydnidae), the anterior lobe is spherical while the posterior is oval (Cossolin et al., 2019). In *P. apterus* (Pyrrhocoridae), the posterior lobe is hand-shaped with four distinct finger-like, but other lobes have an oval shape (Özyurt Koçakoğlu, 2021). There are differences

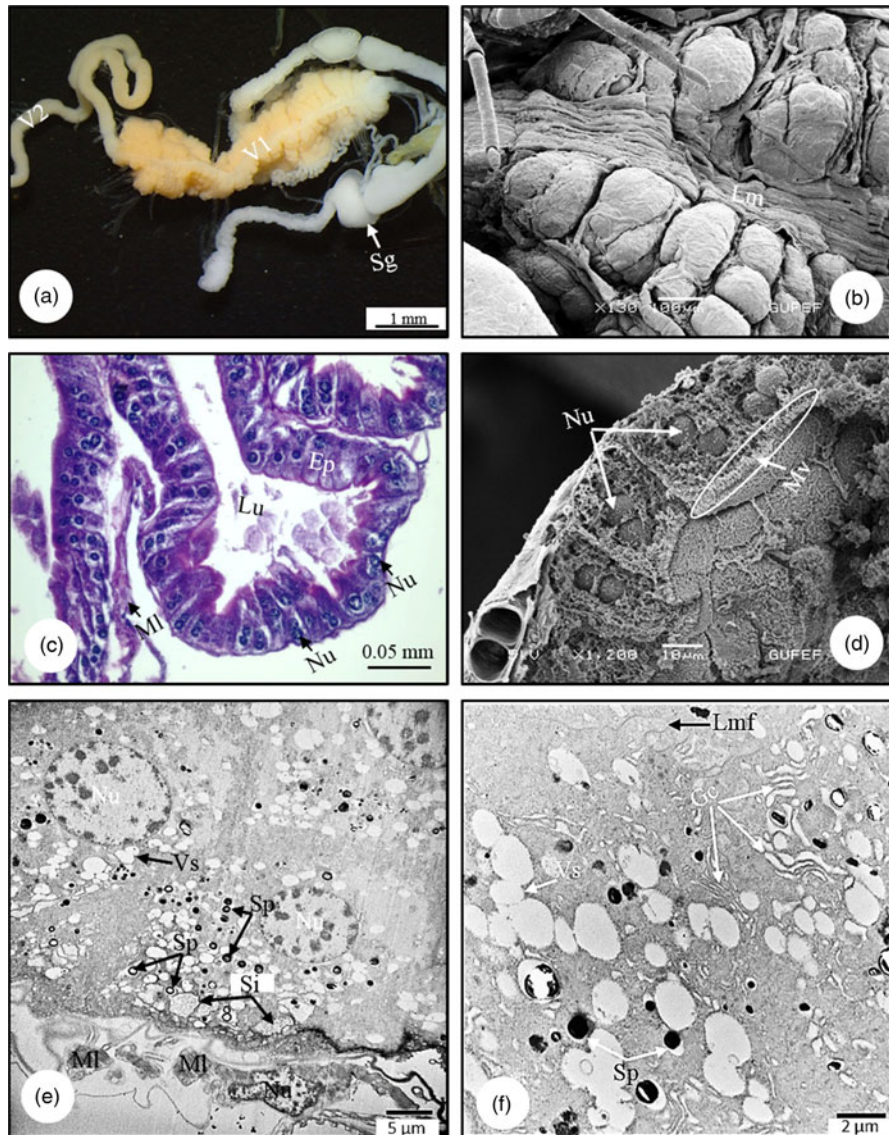


**Fig. 5.** (a) SM photograph of V1 and V2 in *C. mediterraneus*. (b) The longitudinal muscles surrounding gnarled-shaped V1 surface (SEM). (c,d) LM and SEM photographs of the V1 wall which is surrounded by a double-nucleated, monolayered epithelium with round nuclei and sheath. (e) Numerous vesicles, spherocrystals, and cytoplasmic inclusions in the cytoplasm of epithelial cells of V1 (TEM). (f) Golgi complexes, electron-dense, and electron-lucent vesicles in different sizes in the cytoplasm of epithelial cells of V1 (TEM). Ep, epithelium; Gc, Golgi complex; Lmf, lateral membrane folding; Lm, longitudinal muscles; Lu, lumen; MI, muscle layer; Mv, microvilli; Nu, nucleus; Sg, salivary glands; Si, cytoplasmic inclusion; Sp, spherocrystal; V1, ventriculus 1; V2, ventriculus 2; Vs, vesicle.

in the anatomy of salivary glands in different families of the same order or even in different species of the same family.

The type of epithelial cells surrounding the principal gland varies among different species. In *C. mediterraneus*, the principal salivary gland wall is surrounded by a single layer of cuboidal cells. But, in *Notonecta glauca* (Linnaeus, 1758) (Notonectidae), each lobe of principal gland has a single layer of glandular cells in columnar form. The nucleus is large and irregular in shape with fine extensions into the cytoplasm (Baptist, 1941). The epithelial cells of principal salivary gland of *B. tabidus* (Pentatomidae) are flattened (Azevedo et al., 2007). While the epithelium of the anterior lobe of the principal salivary gland of *E. heros* (Pentatomidae) has a single layer of cuboidal cells, the epithelium of the posterior lobe of the principal salivary gland has a single layer of squamous cells (Castellanos et al., 2017).

The contents of the lumen of the principal gland can vary. In *C. mediterraneus*, the principal salivary gland secretion texture is acidophilic and granulous. The lumen content of the principal salivary gland of *E. heros* (Pentatomidae) is basophilic (Castellanos et al., 2017). *Pentatoma rufipes* L. (Pentatomidae), *G. ferrugineus* (Lygaeidae) (anterior and lateral lobes), *Dysdercus howardi* de Geer (Pyrrhocoridae), *P. apterus* (Pyrrhocoridae), and *Corizus parumpunctatus* Schill. (Coreidae), and the anterior lobe secretion took up the basic dye while the posterior lobe took up the acid dye (Baptist, 1941). The composition of saliva in lobes is different between species. It will affect the type of food this species which can digest.

In ultrastructural examinations, the epithelium cytoplasm of principal salivary gland of *C. mediterraneus* has granulated endoplasmic cisternae, mitochondria, electron-lucent structures, and small electron-dense granules characteristic of glycogen deposits

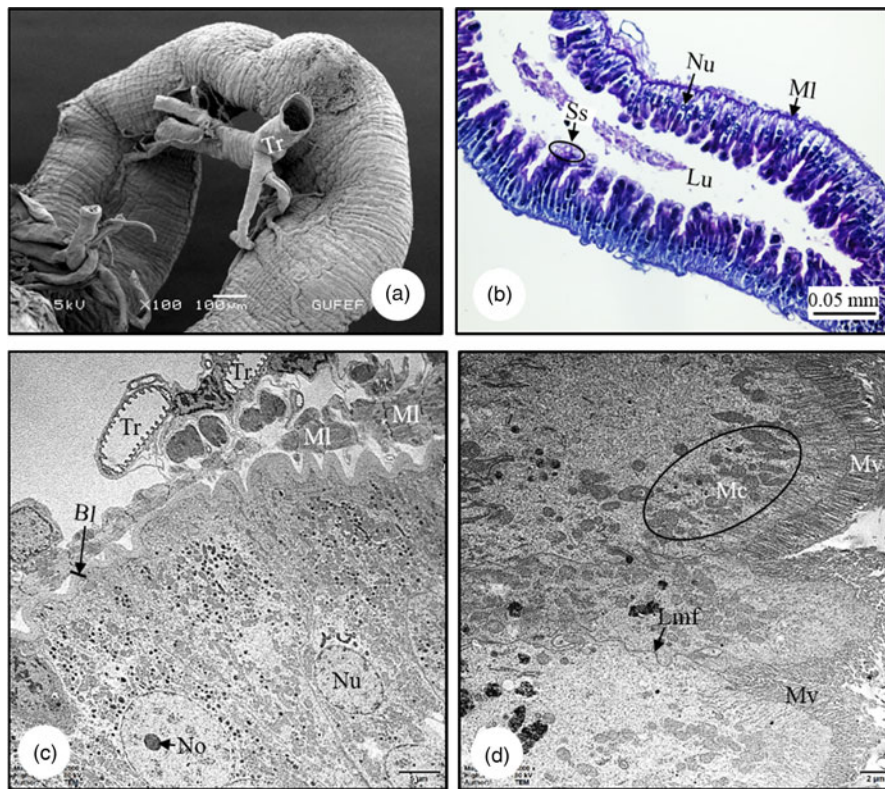


**Fig. 6.** (a) The muscles surrounding long channel shaped V2 in *C. mediterraneus* (SEM). (b) Histological sections of V2 which is surrounded by a monolayer cylindrical epithelium with a round nucleus in the middle, and a thin muscle layer (LM). (c,d) TEM photographs of epithelial cells surrounding V2. Bl, basal lamina; Lmf, lateral membrane folding; Lu, lumen; ML, muscle layer; Mc, mitochondria; Mv, microvilli; No, nucleolus; Nu, nucleus; Ss, secretory sac; Tr, tracheae.

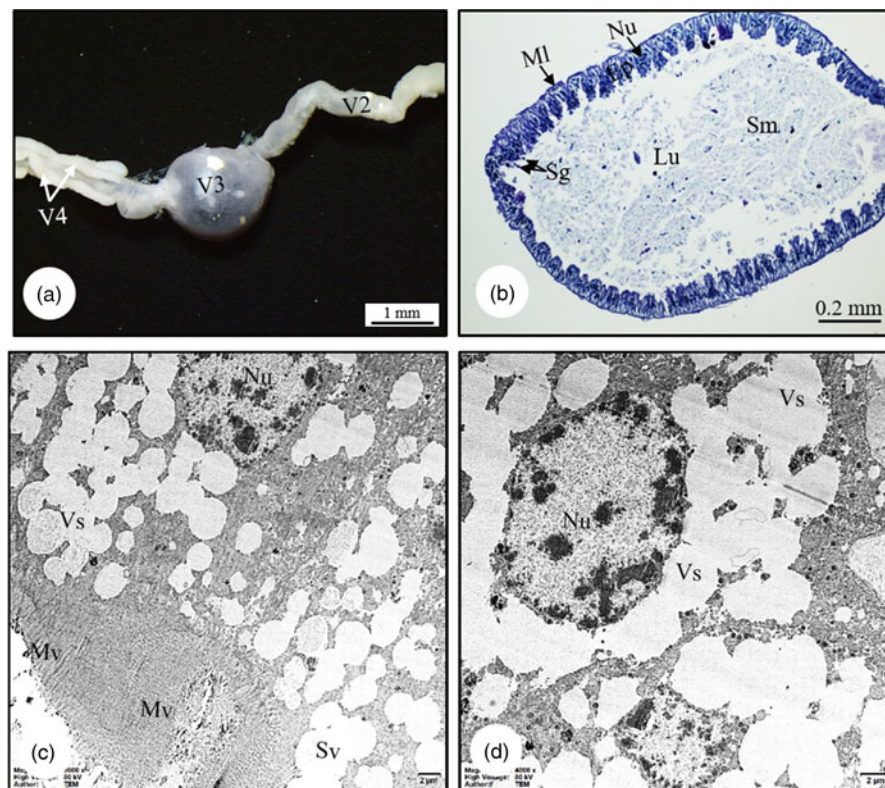


**Fig. 7.** (a) SM photograph of general view in V2 and V3. (b) A monolayer of epithelium and muscle layer surrounding the V3 wall, and a large lumen filled with secretion material (LM). (c,d) TEM photographs of secretory vesicles in epithelial cells surrounding V3. Lu, lumen; ML, muscle layer; Mv, microvilli; Nu, nucleus; Sg, secretory granules; Sm, secretion material; Tr, tracheae; Vs, vesicles; V2, ventriculus 2; V3, ventriculus 3; V4, ventriculus 4.



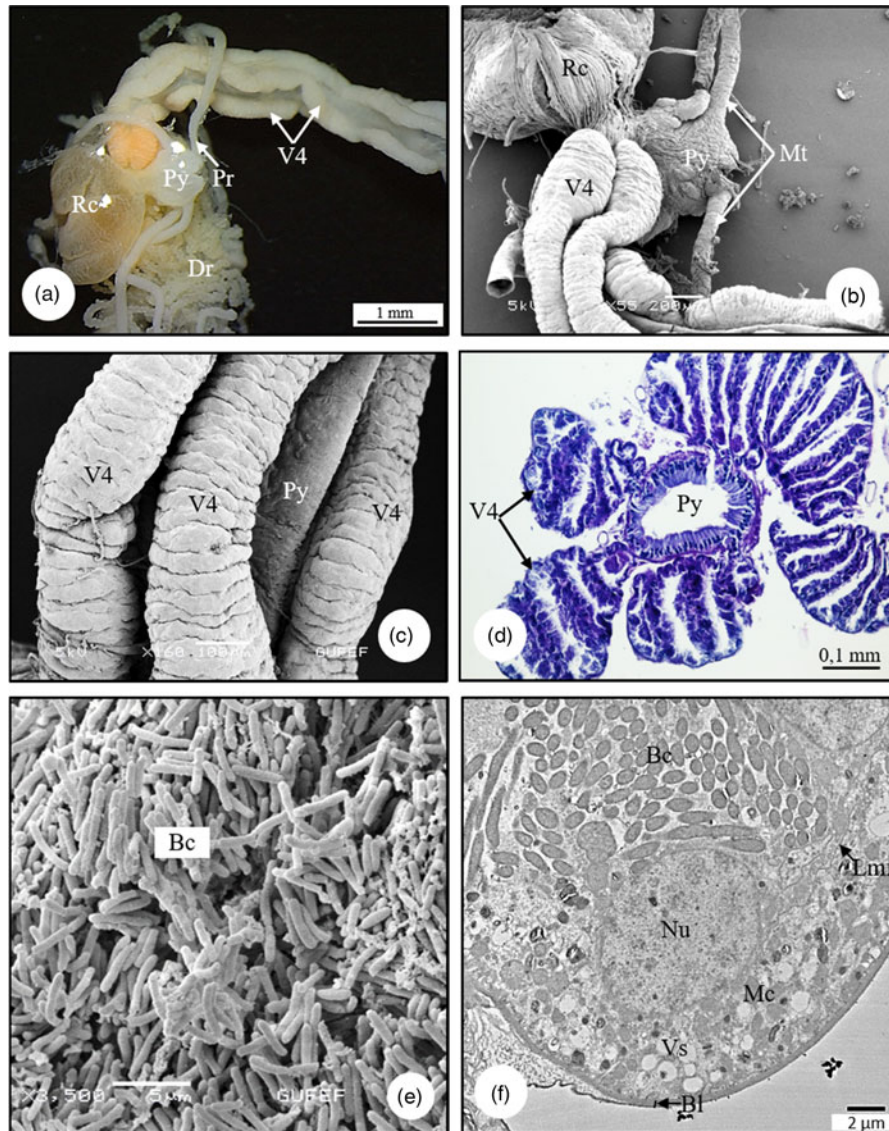


**Fig. 8.** (a,b) SM and SEM photographs of V4, Malpighian tubules, pylorus, and rectum in *C. mediterraneus*. (c) The connection of the V4, which consist of four channels, with the pyloric region (SEM). (d) The cross-section of pylorus and V4 in *C. mediterraneus* (LM). (e) SEM photograph of rod-shaped bacteria in the lumens of V4. (f) The secretion vesicles and mitochondria in cytoplasm of epithelial cells, bacteria in lumen of gastric caeca (TEM). Bc, bacteria; Bl, basal lamina; Dr, distal region; Lmf, lateral membrane folding; Mc, mitochondria; Mt, Malpighian tubule; Nu, nucleus; Pr, proximal region; Py, pylorus; Rc, rectum; V4, ventriculus 4; Vs, vesicle.

as in *E. heros* (Pentatomidae; Castellanos et al., 2017). Besides, the principal gland cytoplasm of salivary gland in *N. glauca* (Notonectidae) contains secretion granules, fine granular and rod-shaped mitochondria, and circular and semi-circular Golgi bodies (Baptist, 1941). In *Lygus* sp., the principal gland cytoplasm has typical mitochondria and granular bodies scattered throughout the cytoplasm (Baptist, 1941). The principal salivary gland cytoplasm of *B. tabidus* (Pentatomidae) has many mitochondria and cisterns of the granulated endoplasmic reticulum (Carvalho et al., 2021). The types of organelles vary in the principal salivary gland of different species.

In *C. mediterraneus*, the muscle layer surrounding the epithelium of the principal salivary gland is distinguished, as in *Peregrinus maidis* Ashmead (Delphacidae) and *Mahanarva fimbriolata* Stål (Cercopidae) and *E. heros* (Pentatomidae) (Ammar, 1986; Nunes & Camargo-Mathias, 2006; Castellanos et al.,

2017). The presence of muscles in the salivary glands may be related to mechanisms underlying salivary transport control, and muscles are likely to contribute to the regulation of secretions released from different parts of the salivary glands.

The wall of the accessory salivary gland of *C. mediterraneus* is surrounded by a monolayer cubic epithelium filled with secretory granules, as in *B. tabidus* (Pentatomidae; Carvalho et al., 2021). In *P. rufipes* (Pentatomidae) and *D. howardii* (Pyrrhocoridae), the accessory salivary gland cells are cubical or columnar, and a cytoplasm has large clear vacuoles. The glandular epithelium of accessory gland in *N. glauca* (Notonectidae) is flattened and devoid of any secretion granules or any special inclusions. In the vesicular type of accessory gland is seen in *N. glauca* (Notonectidae; Baptist, 1941). The type of epithelial cells surrounding the accessory salivary gland varies in different species.

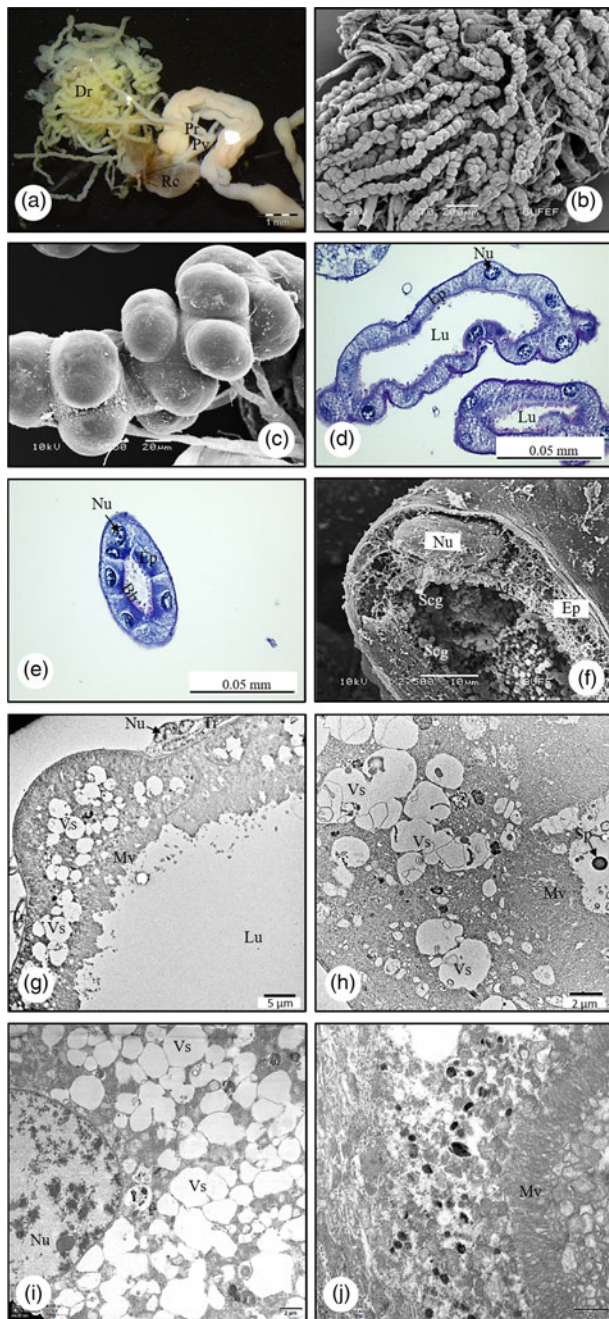


**Fig. 9.** (a) Proximal end of Malpighian tubules which is connected with the pylorus, and distal region of Malpighian tubules which is freely lying in the hemocoel in *C. mediterraneus* (SM). (b) The distal region of Malpighian tubules which is a double string of beads shaped (SEM). (c) SEM photograph of distal region surface of Malpighian tubule. (d,e) The longitudinal and cross-section of Malpighian tubules (LM). (f) The epithelium surrounding Malpighian tubules (SEM). (g–i) Numerous vesicles in various sizes in the cytoplasm of Malpighian tubule cells (TEM). (j) Microvilli extending from the apical of epithelial cells surrounding Malpighian tubules (TEM). Bb, brush border; Dr, distal region; Ep, epithelium; Lu, lumen; Mv, microvilli; Nu, nucleus; Pr, proximal region; Py, pylorus; Rc, rectum; Scg, secretion granules; Sp, spherocrystal; Tr, tracheae; Vs, vesicle.

### Alimentary Canal

The alimentary canal of *C. mediterraneus* is divided into foregut, midgut, and hindgut and a pair of salivary glands and two pairs of Malpighian tubules associated with the alimentary system, as in

*Halys dentatus* (Fabricius, 1775) (Pentatomidae) and *P. apterus* (Pyrrhocoridae) (Gangurde et al., 2019; Özyurt Koçakoglu, 2021).

### Foregut and Midgut

The foregut of *C. mediterraneus* is the first part of the alimentary canal and consists of pharynx and esophagus, as in *Ceroplastes japonicus* Borchsenius 1949 (Coccidae; Xie et al., 2011). Hood (1937) explains that the foregut in *Oncopeltus fasciatus* Dallas (Lygaeidae) consists of pharynx, esophagus, and esophageal valve. *C. mediterraneus* has a thin, long, semi-transparent, tube-shaped esophagus like other heteropteran insects (Hamner, 1936; Hood, 1937; Barber et al., 1980; Özyurt Koçakoglu, 2021).

The number of parts that make up the midgut may differ in interspecifically. Similar to *C. mediterraneus*, the midgut in *Odontopus nigricornis* Stal (Pyrrhocoridae), *Triatoma infestans* Klug, 1835 (Reduviidae), *Dysdercus peruvianus* Guérin-Meneville, 1831, *E. integriceps*, and *H. dentatus* (Pentatomidae) have four regions (Rastogi, 1964; Burgos & Gutiérrez, 1976; Silva et al., 1995; Mehrabadi et al., 2012; Gangurde et al., 2019). However, *Pyrops candelaria* Linn. (Fulgoridae), *B. tabidus* (Pentatomidae), *Cimex hemipterus* Fabricius, 1803 (Cimicidae), and *Podisus nigrispinus* (Dallas 1851) (Pentatomidae) are divided into three ventricles (Cheung & Marshall, 1982; Guedes et al., 2003; Azevedo et al., 2009; Martínez et al., 2018). The midgut of *S. castanea* (Cydnidae) is anatomically divided into five regions (ventricles) (V1–V5). In midgut of *S. castanea* (Cydnidae), V1–V4 regions are similar between males and females, but V5 is different (Cossolin et al., 2020). In *O. fasciatus* (Lygaeidae), the midgut consists of three parts and has a broad stomach at the front, a narrow tubular tube, and a sac-like structure at the very end (Hood, 1937). Cheung & Marshall (1982) and Guedes et al. (2003) divided the midgut of *P. candelaria* (Fulgoridae) and *B. tabidus* (Pentatomidae) into three regions as anterior, middle, and posterior regions. The parts that make up the midgut may differ according to the species.

The shape of midgut epithelial cells differs in interspecifically. The midgut cells of *C. mediterraneus* are arranged in a monolayer cubic and cylindrical shape, as in *O. fasciatus* (Lygaeidae) and *H. dentatus* (Pentatomidae) (Hood, 1937; Gangurde et al., 2019). In *O. nigricornis* (Pyrrhocoridae), the midgut is characterized by the presence of columnar cells (Rastogi, 1964). The V1 in midgut of *S. castanea* (Cydnidae) is formed by a simple columnar epithelium, but the epithelium in V2 and V3 is cubic, the epithelium in V4 is flat. In addition, V5 in male is formed by cubic cells, but the cells of V5 region in the females are large and elongated (Cossolin et al., 2020). In *C. mediterraneus*, V1 epithelium has columnar cells with two nuclei. This was not seen in other parts of the midgut.

The midgut cells of *C. mediterraneus* have a well-developed nucleus with decondensed chromatin and nucleolus, which are the common features of these cells in insects (Billingsley & Lehane, 1996) that occur in cells with high metabolic activity (Alberts et al., 2014). A similar situation was noted in *Coptosoma scutellatum* (Geoffroy, 1785) (Plataspidae), *Graphosoma lineatum* (Linnaeus, 1758) (Pentatomidae), *Rhynocoris iracundus* (Linnaeus, 1758) (Reduviidae), *N. rugosus* (Linnaeus, 1758) (Nabidae), and *H. (Himacerus) apterus* (Fabricius, 1798) (Nabidae) by Santos et al. (2017). Nevertheless, the nuclei of digestive cells occur in *Kleidocerys resedae* (Panzer, 1797)

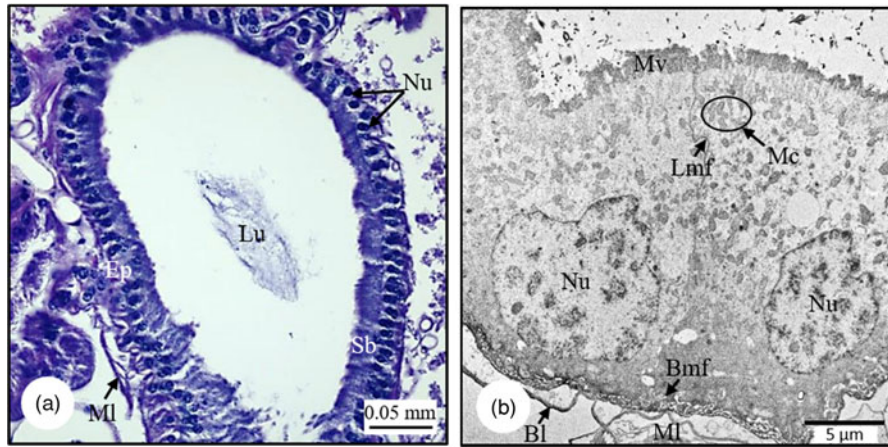


**Fig. 10.** (a) The histological section of pylorus region (LM). (b) The basal membrane folds in the basal part and short microvilli in the apical part of the epithelial cells surrounding pylorus region (TEM). Bl, basal lamina; Bmf, basal membrane folding; Ep, epithelium; Lmf, lateral membrane folding; Lu, lumen; Mc, mitochondria; ML, muscle layer; Mv, microvilli; Nu, nucleus; Sb, striated border.

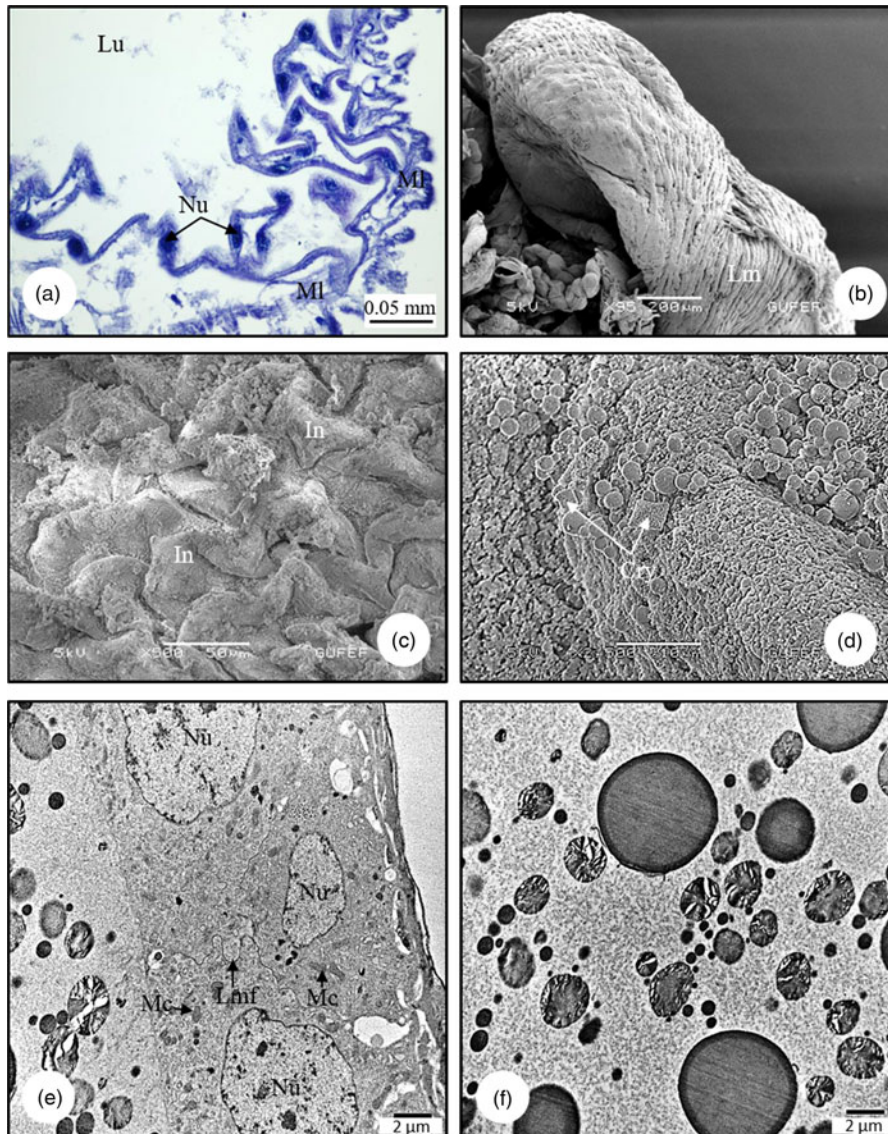


**Fig. 11.** (a) A monolayer of squamous epithelium and muscle layer surrounding the rectum wall in *C. mediterraneus* (LM). (b) SEM photograph of longitudinal muscles on rectum surface. (c) An intima layer with folds on the inner surface of the rectum wall (SEM). (d) Numerous bacteria and square-shaped uric acid crystals which are seen in the lumen of the rectum (SEM). (e) Lateral membrane folding between epithelial cells and numerous mitochondria in cytoplasm (TEM). (f) TEM photograph of bacteria in rectum lumen. Cry, crystal; In, intima; Lmf, lateral membrane folding; Lm, longitudinal muscle; Lu, lumen; Mc, mitochondria; ML, muscle layer; Nu, nucleus.

(Lygaeidae) with some electron-dense patches (Santos et al., 2017).

The ultrastructure of the parts that make up the midgut differs interspecifically. In *C. mediterraneus*, the cytoplasm of midgut epithelial cells involves numerous vesicles, golgi complexes, spherocrystals, and cytoplasmic inclusions. However, in *Spilostethus pandurus* Scop. (Lygaeidae), the cytoplasm of the midgut epithelial cells is packed with mitochondria, granulated endoplasmic reticulum, free ribosomes, lysosomes, and lipid droplets (Meguid et al., 2013). Also, in the perinuclear cytoplasm of digestive cells of *C. scutellatum* (Plataspidae), many spherocrystals and lysosomes (or autophagic structures) were found by Santos et al. (2017). The cytoplasm in V1 of *O. fasciatus* (Lygaeidae) is rich in dark granules, mitochondria, autolysosomes, and lysosomes with electron-dense content, the nucleus rich in decondensed chromatin with clusters of condensed chromatin (Cossolin et al., 2020).

Spherocrystals occur in the cytoplasm of the digestive cells of *C. mediterraneus*. Similar structures were seen in *C. scutellatum* (Plataspidae), *G. lineatum* (Pentatomidae), *R. iracundus* (Reduviidae), *N. rugosus* (Nabidae), and *H. (Himacerus) apterus* (Nabidae) (Santos et al., 2017). The spherocrystals structures store calcium phosphate, magnesium, and potassium; uric acid; iron, cadmium; proteins, and polysaccharides (Cruz-Landim, 1971; Cruz-Landim & Serrão, 1997; Gomes et al., 2012).

In *C. mediterraneus*, V4 is filled with bacteria. Kikuchi et al. (2005) demonstrated symbiotic bacteria in the posterior region of the midgut of *Riptortus clavatus* (Thunberg, 1783) (Alydidae) and *Leptocoris chinensis* (Alydidae). Hirose et al. (2006) show that the gastric cecum of *Nezara viridula* (L.) (Pentatomidae) has *Pantoea* sp. bacteria.

### Malpighian Tubules and Hindgut

Malpighian tubules show a great diversity in number among species. There are four Malpighian tubules in *C. mediterraneus*, as in *T. infestans* (Reduviidae) and *D. baccarum* (Mello & Dolder, 1977; Özyurt et al., 2017). However, *C. japonicus* (Coccidae) has two Malpighian tubules (Xie et al., 2011). Besides, there are four to six Malpighian tubules in *Eurygaster integriceps* Puton, 1881 (Hemiptera: Scutelleridae; Mehrabadi et al., 2012).

The color of Malpighian tubules differs interspecifically. In *C. mediterraneus*, they are light yellow; however, in *C. japonicus* (Coccidae), Malpighian tubules consist of brownish-yellowish tubes with pores on them, and there are many crystals and long microvilli inside the tubes (Xie et al., 2011). Also, the proximal region of Malpighian tubules in *P. apterus* (Pyrrhocoridae) looks brown, and distal region looks green (Özyurt Koçakoğlu, 2021). In *C. mediterraneus*, Malpighian tubules consist of two regions as proximal and distal regions. The proximal end of these tubes are in the form of a straight channel while the distal parts are bead-shaped and their ends are closed, lying freely in the body cavity, as in *P. apterus* (Özyurt Koçakoğlu, 2021).

The spherocrystals are situated in the Malpighian tubule lumen of *C. mediterraneus*. These structures are also seen in *D. baccarum* (Özyurt et al., 2017). The spherocrystals store products of mineral and organic materials, regulating the maintenance of proper mineral composition and the accumulation of nontoxic waste materials and toxic metals (Chapman, 2013).

As in *C. japonicus* (Coccidae) and *P. apterus*, the hindgut of *C. mediterraneus* consists of two parts, the pylorus and the rectum (Xie et al., 2011; Özyurt Koçakoğlu, 2021). However, in *Abedus ovatus* (Stal) (Belostomatidae), the hindgut includes ileum, rectal

cecum, and rectum (Goverdhan et al., 1981). In addition, the hindgut of *H. dentatus* (Pentatomidae) consists of anterior intestine, rectal sac, and anal canal (Gangurde et al., 2019). In pylorus of *C. mediterraneus*, there is a unique type epithelial cell and the cells are equal in length. However, the pylorus in *Abedus ovatus* (Stal) (Belostomatidae) has two types of epithelium, normal and membranous epithelium (Goverdhan et al., 1981). In the posterior part of the pylorus, the normal epithelium is taller than those of the anterior region. Unlike the muscles surrounding the pylorus of *C. mediterraneus*, the muscles surrounding pylorus of *A. ovatus* (Belostomatidae) are rather poorly developed (Goverdhan et al., 1981). The parts of the hindgut differ according to the species.

Histologically, the shape of the cells surrounding rectum in different species have cylindrical, cubic, and flat shapes. In *C. mediterraneus*, the rectum wall is surrounded by a monolayer of squamous epithelium. The rectum of *P. apterus* is surrounded by cuboidal epithelial cells (Özyurt Koçakoğlu, 2021). In the rectum of *C. mediterraneus*, there is a unique type epithelial cell, as in *P. apterus*. However, Harris (1938) states that there are two cells in the epithelium of rectal sac in *Murgantia histrionica* (Hahn, 1834) (Pentatomidae). Similar to *P. apterus*, in the rectum lumen of *C. mediterraneus*, there are crystals (Özyurt Koçakoğlu, 2021). Ultrastructurally, in the rectum of *C. mediterraneus*, epithelial cells have numerous mitochondria. However, in *Cenocorixa bifida* (Hungerford, 1926) (Corixidae), ultrathin sections of the rectum show granular cytoplasm and very few small mitochondria (Jarial, 1964).

In conclusion, the aim of this article was to obtain information on the alimentary canal biology of species belonging to Pentatomidae and other families, to be useful for future studies on Heteroptera taxonomy and phylogeny, and also to form a basis for future studies on the biological control of this species.

**Acknowledgments.** We thank Gazi University, BAP, for the support of this research (Grant FGA-2021-7176). The author's thanks are also extended to Gazi University Academic Writing Center for the proofreading of this paper.

**Conflict of interest.** The authors declare that they have no conflict of interest disclosed in this work.

**Additional information.** This article was originally submitted by the authors in English and is first published here.

### References

- Alberts B, Johnson A, Lewis J, Morgan D, Raff M, Roberts K & Walter P (2014). *Molecular Biology of the Cell*, 6th ed. New York: Garland Science.
- Ammar ED (1986). Ultrastructure of the salivary glands of the planthopper, *Peregrinus maidis* (Ashmead) (Homoptera: Delphacidae). *Int J Insect Morphol Embryol* 15, 417–428.
- Anhê ACBM, Maia Godoy RS, Nacif-Pimenta R, Barbosa WF, Lacerda MV, Monteiro WM, Secundino NFC & Paolucci Pimenta PF (2021). Microanatomical and secretory characterization of the salivary gland of the *Rhodnius prolixus* (Hemiptera, Reduviidae, Triatominae), a main vector of Chagas disease. *Open Biol* 11(6), 210028.
- Azevedo DDO, Neves CA, Mallet JRS, Gonçalves TCM, Zanuncio JC & Serrão JE (2009). Notes on midgut ultrastructure of *Cimex hemipterus* (Hemiptera: Cimicidae). *J Med Entomol* 46, 435–441.
- Azevedo DDO, Zanuncio JC, Zanuncio JS Jr, Martins GF, Marques-Silva S, Sossai MF & Serrão JE (2007). Biochemical and morphological aspects of salivary glands of the predator *Brontocoris tabidus* (Heteroptera: Pentatomidae). *Braz Arch Biol Technol* 50, 469–477.
- Baptist BA (1941). The morphology and physiology of the salivary glands of Hemiptera-Heteroptera. *J Cell Sci* 2(329), 91–139.

- Barber DT, Cooksey LM & Abell DW (1980). Study of the anatomy of the alimentary canal of *Brochymena quadripustulata* (Hemiptera: Pentatomidae). *J Ark Acad Sci* **34**(1), 16–18.
- Billingsley PF & Lehane MJ (1996). Structure and ultrastructure of the insect midgut. In *Biology of the Insect Midgut*, Billingsley PF & Lehane MJ (Eds.), pp. 3–30. London: Chapman & Hall.
- Burgos MH & Gutiérrez LS (1976). The intestine of *Triatoma infestans*. I. Cytology of the midgut. *J Ultrastruct Res* **57**, 1–9.
- Candan S, Özyurt Koçakoğlu N & Serttaş A (2021). Histoanatomy of Malpighian tubules and the digestive tract of adult of biocontrol agent *Calosoma sycophanta* L. (Coleoptera: Carabidae). *Int J Trop Insect Sci* **41** (2), 1373–1386.
- Carvalho PEGR, Martínez LC, Cossolin JFS, Plata-Rueda A, Jumbo LOV, Fiaz M, Carvalho AG, Zanuncio JC & Serrão JE (2021). The salivary glands of *Brontocoris tabidus* (Heteroptera: Pentatomidae): Morphology and secretory cycle. *Tissue Cell* **70**, 101498.
- Castellanos N, Martínez LC, Silva EH, Teodoro AV, Serrão JE & Oliveira EE (2017). Ultrastructural analysis of salivary glands in a phytophagous stink bug revealed the presence of unexpected muscles. *PLoS One* **12**(6), e0179478.
- Chapman RF (2013). The excretory system: Structure and physiology. In *Comprehensive Insect Physiology Biochemistry and Pharmacology, Regulation, Vol. 4: Digestion, Nutrition, Excretion*, Kerkut GA & Gilbert LI (Eds.), pp. 421–466. Oxford, UK: Pergamon Press.
- Cheung WWK & Marshall AT (1982). Ultrastructural and functional differentiation of the midgut of the lantern bug, *Pyrops candelaria* Linn. (Homoptera: Fulgoridae). *Cytologia* **47**, 325–339.
- Cossolin JFS, Lopes DRG, Martínez LC, Santos HCP, Fiaz M, Pereira MJB, Vivian LM, Mantovani HC & Serrão JE (2020). Morphology and composition of the midgut bacterial community of *Scaevola castanea* Perty, 1830 (Hemiptera: Cydnidae). *Cell Tissue Res* **382**, 337–349.
- Cossolin JFS, Martínez LC, Pereira MJB, Vivian LM, Bozdoğan H, Fiaz M & Serrão JE (2019). Anatomy, histology, and ultrastructure of salivary glands of the burrower bug, *Scaevola castanea* (Hemiptera: Cydnidae). *Microsc Microanal* **25**(6), 1482–1490.
- Cruz-Landim C (1971). Note on granules with concentric lamination present in the larval midgut of *Trigona (Scaevola) portico* Latr. (Hymenoptera: Apidae). *Rev Bras Pesqui Med Biol* **4**, 13–16.
- Cruz-Landim C & Serrão JE (1997). Ultrastructure and histochemistry of the mineral concretions in the midgut of bees (Hymenoptera: Apidae). *Neth J Zool* **47**, 21–29.
- Dantas PC, Serrão JE, Santos HCP & Carvalho GA (2021). Anatomy and histology of the alimentary canal of larvae and adults of *Chrysoperla externa* (Hagen, 1861) (Neuroptera: Chrysopidae). *Arthropod Struct Dev* **60**, 101000.
- Fent M & Aktaş N (1999). Edirne yöresi Pentatomidae (Heteroptera) faunası üzerine taksonomik ve faunistik araştırmalar. *Turk J Zool* **23**(2), 377–395.
- Gangurde JH, Gurule SA & Tidame SK (2019). Anatomy and histopathology of alimentary canal of *Halys dentatus* (Hemiptera: Pentatomidae) treated with dichlorovos. *Indian J Appl Res* **9**(10), 61–66.
- Gomes FM, Carvalho DB, Peron AC, Saito K, Miranda K & Machado EA (2012). Inorganic polyphosphates are stored in spherites within the midgut of *Anticarsia gemmatalis* and play a role in copper detoxification. *J Insect Physiol* **58**, 211–219.
- Goverdhan TL, Shyamasundari K & Rao KH (1981). Histology and histochemistry of the alimentary canal of *Abedus ovatus* (Stal) (Heteroptera: Belostomatidae). *Proceed: Anim Sci* **90**(2), 237–251.
- Guedes BAM, Serrão JE, Zanuncio JC & Neves CA (2003). Morphology of the midgut in the predatory sting bug *Brontocoris tabidus* (Heteroptera: Pentatomidae). *XIX Congress of the Brazilian Society for Microscopy and Microanalysis*, pp. 101–102. Brezilya.
- Gullan PJ & Cranston PS (2005). *The Insects: An Outline of Entomology*, 3rd ed. Oxford: Blackwell Publishing.
- Hamner AL (1936). The gross anatomy of the alimentary canal of *Solubea pugnax* (Fab.) (Heteroptera, Pentatomidae). *Ohio J Sci* **36**(3), 157–160.
- Hirose E, Panizzi AR, De Souza JT, Cattelan AJ & Aldrich JR (2006). Bacteria in the gut of southern green stink bug (Heteroptera: Pentatomidae). *Ann Entomol Soc* **99**(1), 91–95.
- Hood CW (1937). The anatomy of the digestive system of *Oncopeltus fasciatus* Dall. (Heteroptera: Lygaeidae). *Ohio J Sci* **37**(3), 151–160.
- Jarial MS (1964). Histophysiological and ultrastructural studies on the hindgut and brain of *Cenocorixa bifida* (Hemiptera-Insecta). MSc Thesis. The University of British Columbia, England.
- Kasap H (1979). A comparative anatomical study of the alimentary canal of Chrysomelidae (Coleoptera: Polyphaga). *Fen Fak Tebliğler Derg* **22**, 53–78.
- Kikuchi Y, Meng XY & Fukatsu T (2005). Gut symbiotic bacteria of the genus *Burkholderia* in the broad-headed bugs *Riptortus clavatus* and *Leptocoris chinensis* (Heteroptera: Lygaeidae). *Appl Environ Microbiol* **71**(7), 4035–4043.
- Klowden MJ (2007). *Physiological Systems in Insects*, 2nd ed. San Diego, USA: Academic Press.
- Martínez LC, Plata-Rueda A, da Silva Neves G, Gonçalves WG, Zanuncio JC, Bozdoğan H & Serrão JE (2018). Permethrin induces histological and cytological changes in the midgut of the predatory bug, *Podisus nigripinus*. *Chemosphere* **212**, 629–637.
- Meguid AA, Awad HH, Omar AH & Elelimy HA (2013). Ultrastructural study on the midgut regions of the milkweed bug, *Spilostethus pandurus* Scop. (Hemiptera: Lygaeidae). *Asian J Biol Sci* **6**(1), 54–66.
- Mehrabadi M, Bandani AR, Allahyari M & Serrão JE (2012). The Sunn pest, *Eurygaster integriceps* Puton (Hemiptera: Scutelleridae) digestive tract: Histology, ultrastructure and its physiological significance. *Micron* **43**, 631–637.
- Mello MLS & Dolder H (1977). Fine structure of the Malpighian tubes in the blood-sucking insect, *Triatoma infestans* Klug. *Protoplasma* **93**, 275–288.
- Nunes PH & Camargo-Mathias MI (2006). Ultrastructural study of the salivary glands of the sugarcane spittlebug *Mahanarva fimbriolata* (Stal, 1854) (Hemiptera: Cercopidae). *Micron* **37**, 57–66.
- Önder F, Karsavuran Y, Tezcan S & Fent M (2006). *Türkiye Heteroptera (Insecta) Kataloğu*. İzmir: Meta Basım.
- Önder F & Lodos N (1986). Preliminary list of Tingidae with notes on distribution and importance of species in Turkey. *Rev Appl Entomol* **71** (7), 46–59.
- Özyurt N, Amutkan D, Polat I, Kocamaz T, Candan S & Suludere Z (2017). Structural and ultrastructural features of the Malpighian tubules of *Dolycoris baccarum* (Linnaeus 1758) (Heteroptera: Pentatomidae). *Microsc Res Technol* **80**(4), 357–363.
- Özyurt Koçakoğlu N (2021). Morphology and histology of the alimentary canal, salivary glands and Malpighian tubules in *Pyrrhocoris apterus* (Linnaeus, 1758) (Hemiptera: Pyrrhocoridae): a scanning electron and light microscopies study. *Int J Trop Insect Sci* **41**(2), 1845–1862.
- Özyurt Koçakoğlu N & Candan S (2021). Characterization of the alimentary canal and Malpighian tubules of *Chrysolina herbacea* (Duftschmid, 1825) (Coleoptera: Chrysomelidae): Anatomical and histological approaches. *Microsc Res Technol* **84**(6), 1135–1144.
- Rastogi SC (1964). Studies on the digestive system of *Odontopus nigricornis* Stal (Hemiptera, Pyrrhocoridae). *Tijdschr Ent* **107**, 265–275.
- Santos HP, Rost-Roszkowska M, Vilimova J & Serrão JE (2017). Ultrastructure of the midgut in Heteroptera (Hemiptera) with different feeding habits. *Protoplasma* **254**(4), 1743–1753.
- Silva CP, Ribeiro AF, Gulbenkian S & Terra WR (1995). Organization, origin and function of the outer microvillar (perimicrovillar) membranes of *Dysdercus peruvianus* (Hemiptera) midgut cells. *J Insect Physiol* **41**, 1093–1103.
- Xie Y, Liu W, Zhang Y, Xiong Q, Xue J & Zhang X (2011). Morphological and ultrastructural characterization of the alimentary canal in Japanese wax scale (*Ceroplastes japonicus* Green). *Micron* **42**(8), 898–904.